

# Microstructure Engineering to Optimize Hardness and Conductivity in Electrolytic Tough Pitch Copper



N. HARSHAVARDHANA, M.P. GURURAJAN, and PRITA PANT

Extensive investigations were carried out on the mechanical strength, electrical conductivity, and microstructure of commercially pure copper, which was rolled at room temperature to deformations less than 23 pct and subsequently heat treated at a range of temperatures less than  $0.5T_m$ . For various reductions in samples thickness, we have identified the optimum heat treatment temperature that yields higher mechanical strength and electrical conductivity than the as-received sample. Specifically, with increasing deformation, the optimum heat treatment temperature decreases. We are able to correlate the properties with the microstructure which is composed of deformed grains that enhance strength and the relatively deformation-free grains that enhance electrical conductivity. More importantly, the optimum properties are achieved when the volume fraction of the relatively deformation-free grains are in the range 65 to 70 pct. We also show that the grain orientation spread obtained using electron back-scattered diffraction is ideal, in these studies, to distinguish between deformed and relatively deformation-free grains.

<https://doi.org/10.1007/s11661-019-05315-9>

© The Minerals, Metals & Materials Society and ASM International 2019

## I. INTRODUCTION

ELECTROLYTIC tough pitch (ETP) copper is commercially pure, high-conductivity copper. It is used for motor and transformer windings, residential wiring, electrical cables, and bus bars. Among these, motor and transformer windings and residential wiring (called building wire) require high strength, along with conductivity higher than 100 pct IACS, preferably reaching 102 pct IACS.<sup>[1,2]</sup> If conductivity can be improved without loss in strength, it will improve efficiency and reduce losses. Hence, there exist several studies focusing on either conductivity or strength with specific reference to the effect of defects on these properties.

Electrical conductivity of metals depends on electron mobility and the distance which electrons can cover without scattering off any obstacles present. The obstacles typically present in the path of the electrons are impurity atoms, vacancies, dislocations, and internal boundaries—such as grain or phase boundaries. They lead to a decrease in conductivity, or, a rise in the inverse of conductivity, called resistivity. Total

resistivity ( $\rho$ ) can be expressed as a sum of resistivities, each accounting for a different type of obstacle. This relation is called Matthiessen's law:  $\rho = \rho_t + \rho_I + \rho_d + \rho_b$ .<sup>[3]</sup> In the case of commercially pure metals, the contributions of dislocations ( $\rho_d$ ), temperature ( $\rho_t$ ), and internal boundaries ( $\rho_b$ ) are significant, while the impurity contribution ( $\rho_I$ ) is negligible. On the other hand, in general, the defects that reduce conductivity (by scattering electrons moving through the crystal) lead to enhanced mechanical strength by impeding the movement of dislocations. Specifically, impurity atoms, dislocations, and boundaries lead to solute, work, and boundary strengthening, respectively. Hence, reports of a combination of high mechanical strength and high electrical conductivity are rare—but they do exist. For example, a combination of 95 pct International Annealed Copper Standard (IACS) conductivity and 610 MPa yield strength is reported in Reference 4, while  $96.9 \pm 1.1$  pct IACS conductivity and 900 MPa yield strength is observed in electrodeposited samples.<sup>[5]</sup> Typically, samples with both high strength and high conductivity require specialized processing, such as high strain rate deformation at liquid nitrogen temperatures<sup>[4]</sup> or electrodeposition.<sup>[5]</sup> Such high strength and high conductivity combination is attributed to either bimodal grain structures or to the combined effects of ultrafine grains and optimal size and spacing of twins in these reports.

Other processes such as severe plastic deformation followed by heat treatment do lead to higher yield strengths in the range from 280 to 350 MPa, but

M.P. GURURAJAN and PRITA PANT are with the Department of Metallurgical Engineering and Materials Science, Indian Institute of Technology Bombay, Powai, Mumbai 400076 India. Contact e-mail: [pritapant@iitb.ac.in](mailto:pritapant@iitb.ac.in) N. HARSHAVARDHANA is with the Department of Mechanical Engineering, SRM Institute of Science and Technology, Kattankulathur, Kancheepuram, Tamil Nadu 603 203, India.

Manuscript submitted July 24, 2018.

Article published online June 11, 2019

conductivity is reduced to 81 from 94.5 pct IACS.<sup>[6–8]</sup> For example, Habibi *et al.*<sup>[7]</sup> showed that by obtaining bimodal grain size, strength and electrical conductivity of pure copper are proportionately increased. This increase in strength is attributed to the formation of fine grains due to partial recrystallization. Conductivity was found to be 98, 81, and 89 pct IACS, respectively, for coarse-grained, deformed, and deformed and annealed samples. Similarly, Higuera and Cabrera<sup>[8]</sup> reported that a combination of large recrystallized grains and smaller heavily deformed grains resulted in a combination of high strength and reasonably high conductivity in ETP copper. Heavy deformation and the heat generated during deformation was sufficient to cause both static and dynamic recrystallization, resulting in the bimodal microstructure, which lead to a UTS of about 400 MPa with only a 1.28 pct reduction in conductivity.

From these studies, it is clear that the combination of high strength with attendant small loss in conductivity is due to an optimized, composite microstructure of strained grains (which enhance mechanical strength) and the strain-free grains (which enhance conductivity). This leads to the question whether such an optimized microstructure can be achieved by conventional thermomechanical processing methods (which are more amenable to bulk production processes—such as rolling and heat treatment, for example). In this paper, we show that it indeed is possible to achieve such optimal microstructures by using a process similar to the strain recrystallization (or strain annealing) methodology described in, for example, Kumar *et al.*<sup>[9]</sup> In addition, we also identify the microstructural measures that indicate the optimized microstructure that help us enhance strength with no loss in conductivity.

## II. EXPERIMENTAL DETAILS

Samples of commercially pure polycrystalline ETP copper (LME Grade A, 99.96 pct purity) were obtained from our industrial partner. According to the materials specification sheets provided by our industrial partner, the samples contained trace amounts of impurities, as shown in Table I. These samples were subjected to relatively low amounts of deformation (namely, 2.9, 5.2, 8.7, 12.1, 15.9, and 22.5 pct reduction in thickness) by room-temperature rolling. The rolled samples were heat treated for two hours at temperatures ranging from 150 °C to 300 °C (in 10 °C intervals).

Subsequent to the thermomechanical treatment, the sample surfaces (size 15 mm × 15 mm) were prepared by paper polishing using 220, 400, 600, 1000, 2500, and 4000 grade SiC papers, rotating the polished surface of the sample by 90 deg after each change of paper. After

**Table I. Impurities in As-Received Sample (in ppm)**

Te	Se	Bi	Sb	As	Sn	Pb	Fe	Ni	S	Ag
0.2	0.2	0.1	0.2	0.21	0.1	0.1	1.21	0.68	5.10	11.9

the paper polish, conductivity measurements are carried out. Paper-polished samples were subjected to diamond polishing with 1-micron-grade diamond paste with HIFIN™ lubricant at a rotation rate of 300 rpm. At the end of this process a mirror finish surface is obtained, on which hardness measurements are carried out. An additional electropolishing step was required for EBSD scans. Electropolishing was carried out at room temperature and at 15 V, using an electrolyte consisting of 10 pct orthophosphoric acid, 30 pct ethanol, and 60 pct distilled water.

The electrical conductivity measurements were carried out using an eddy current tester operated at an applied frequency of 60 kHz. A minimum of 25 measurements at various locations were made on each sample to obtain the average conductivity value.

The hardness measurements were carried out as per ASTM E18 using a universal hardness testing machine. Hardness values are represented using HRF (Rockwell F scale). At least 8 measurements at different points were taken to obtain the average hardness value.

From these hardness values, it is possible to obtain an estimate of expected values of yield strength. This is done by converting the hardness from HRF to Vickers ( $H_V$ ) using ASTM E140, and using a relation of the form  $\sigma_y \propto H_V$ . It has been shown that the proportionality constant is dependent on the material and the extent of deformation.<sup>[10]</sup> In our experiments, the ratio of yield strength to hardness varies from about 2.3 for samples with 71 HRF to 2.8 for samples with 90 HRF, since we have measured yield strengths of 175 to 301 MPa in these two cases, respectively. Even though we report hardness in HRF for the rest of this paper, these yield strength values and the conversion factor indicated here might be helpful in estimating the expected yield strength values in our optimized samples.

FEI Quanta-200HV SEM (Scanning Electron Microscope) was used to obtain EBSD (Electron Back Scatter Diffraction) microstructures. Typically, EBSD scans of  $250 \times 250 \mu\text{m}^2$  were carried out with 0.3  $\mu\text{m}$  step size. Further EBSD analyses for the microstructural measures, namely, Grain Average Misorientation (GAM), Kernel Average Misorientation (KAM), and Grain Orientation Spread (GOS), were done using TSL-OIM™ EBSD package.

## III. RESULTS AND DISCUSSION

In Figure 1, we show the Inverse Pole Figure (IPF) map obtained from EBSD for the as-received ETP (LME Grade A) copper. Grain boundaries are marked as black lines, and colors in the IPF map correspond to orientations, as per the standard IPF shown. Grains were defined as being surrounded by a continuous boundary, with misorientation across the boundary being greater than 5 deg. To ensure reliability of data, only points with confidence index,  $CI > 0.1$  ( $CI$  is an indicator of the accuracy with which the software indexes the Kikuchi bands), were considered for analysis and grains less than 3 pixels in size were discarded. The mean grain size for this material is  $11.4 \pm 3.5$  microns;

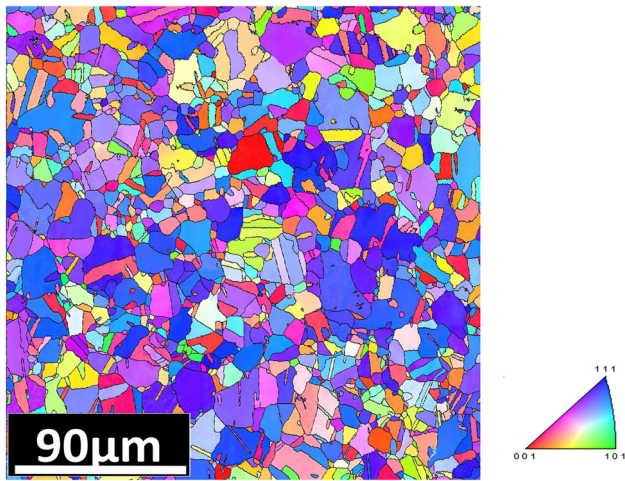


Fig. 1—The inverse pole figure (IPF) map of the as-received sample. The average grain size is  $11.4 \pm 3.5 \mu\text{m}$ . The average hardness and conductivity of this sample are  $51.8 \pm 1.1$  (on Rockwell F Scale) and  $101.3 \pm 0.1$  pct IACS, respectively.

the conductivity is  $101.3 \pm 0.1$  pct IACS (International Association for Copper Standard) and the hardness is  $51.8 \pm 1.1$  on Rockwell F Scale. Mean grain sizes were calculated using area fraction, typically considering 100 to 600 grains.

In Figure 2, we summarize (a) the hardness and (b) the conductivity of copper samples subjected to different percentage deformation (described in terms of percentage reduction in thickness) followed by heat treatment at various temperatures for two hours. In Figure 2(c), the temperature at which hardness and conductivity values undergo sharp changes is plotted for various percentage deformations. In this set of experiments, samples are subjected to room-temperature rolling (*i.e.*, 7.9, 20.5, 33.0, and 39.9 pct reduction in thickness) followed by isochronal heat treatment (for 2 hours) from 150 °C to 250 °C with a step size of 10 °C.

At the low end of heat treatment temperatures (up until 180 °C), there is neither reduction in hardness nor increase in conductivity. However, heat treatment at the higher end of temperatures (in the 210 °C to 250 °C window) results in conductivity reaching a maximum of about 102.1 pct IACS and hardness reaching a minimum of about 30 HRF.

In the intermediate range, when the heat treatment is performed between 180 °C and 210 °C, for samples with deformation more than 20 pct (namely, 20.5, 33.0, and 39.9 pct), the drop in hardness is sudden (from 85 HRF to 35 HRF) and the increase in conductivity is steep (from 99.3 to 102.1 pct IACS). On the other hand, in the case of 7.9 pct deformed sample, at these intermediate temperatures (180 °C to 210 °C), there is an increase in conductivity (from 100.4 pct IACS to 101.3 pct IACS) without any appreciable reduction in hardness (which remains at 76 HRF). From Figure 2(c), it is clear that though the temperature at which hardness drops sharply, decreases with increasing deformation, the temperature at which conductivity increases sharply remains nearly constant. Further, the temperature at

which hardness and conductivity change, are the same for 20 pct and higher deformations.

Based on this set of experiments, we decided to restrict deformations to about 20 pct followed by isochronal heat treatment (for 2 hours) at intermediate temperatures (180 °C to 210 °C) since such a process results in better strength than the as-received material while recovering conductivity to the as-received levels. Hence, in this paper, we present results from the set of experiments in which the deformation was restricted to about 22.5 pct. This choice of percentage deformation and temperatures of anneal, of course, is crucially dependent on the time of heat treatment, namely, 2 hours that we have chosen.

In Figure 3, we show the hardness and conductivity of copper samples (normalized by the as-received values, namely 51.8 HRF and 101.3 pct IACS) subjected to different percentages of reduction in thickness and then heat treated at various temperatures for two hours. The hardness as well as the conductivity of 2.9 and 5.2 pct deformed samples showed nearly identical variation for the entire range of heat treatment temperatures. Hence, for the remainder of this paper, we only report results from the sample deformed to 2.9 pct. For samples deformed to 8.7, 12.1, 15.9, and 22.5 pct, as expected, with increasing deformation, the hardness of the deformed sample increases while the conductivity decreases. If the temperature of heat treatment is low, neither hardness nor conductivity changes. At the higher temperatures shown in Figure 3, though conductivity increases (about 0.2 to 0.6 pct more than the as-received sample), hardness drops precipitously (by about 40 pct as compared to as-received sample). There is an intermediate range of temperatures for which the hardness remains nearly the same as the as-deformed value, while the conductivity starts to increase. This is clearly visualized from Figure 3(f) which shows that changes in conductivity begin at lower temperatures than hardness, providing a window of heat treatment temperatures over which conductivity can be improved, while still obtaining high hardness. This difference in change point temperatures is about 30 °C for lower deformations, and decreases to 10 °C for the 15.9 pct deformed samples. We note that the sample deformed to 22.5 pct is different in this respect; here, the hardness starts dropping as early as 160 °C while the recovery of conductivity does not start up until 180 °C, indicating that the changes in microstructure that lead to recovery of hardness and conductivity might be different from those in samples with less reduction in thickness. Since our interest lies in simultaneous improvement of both hardness and conductivity, in the following discussion we will focus on samples that have been deformed to 15.9 pct or less.

In order to understand the microstructural changes that correspond to the observed changes in hardness and conductivity, we have carried out microstructural studies using EBSD. Even though the effects of cold rolling on mechanical properties,<sup>[11,12]</sup> and on microstructures are widely studied,<sup>[12–22]</sup> they all focus on large deformation followed by recrystallization. Our interest in this study is in deformation less than about 22 pct.

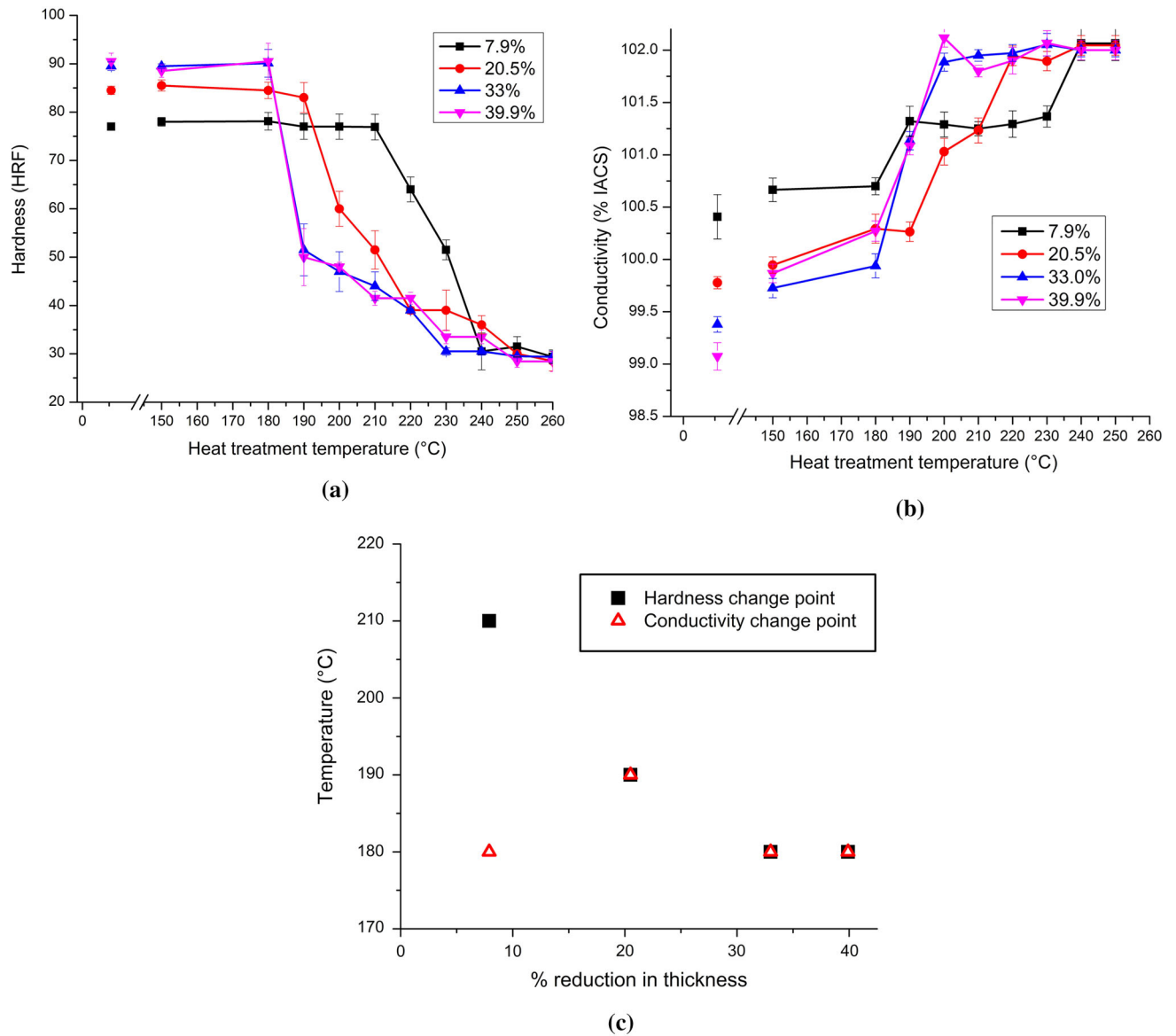


Fig. 2—Variation of (a) hardness and (b) conductivity with isochronal annealing temperature after deformation of 7.9, 20.5, 33.0, and 39.9 pct reduction in thickness. The as-deformed values are the individual points. (c) The temperatures at which hardness and conductivity show a significant change in values. The lines drawn through the data points of heat-treated samples are only a guide to the eye.

Specifically, for 2.9, 8.7, 12.1, and 15.9 pct deformation, we have identified four types of samples: (A) as-deformed, (B) samples exhibiting negligible change in hardness or conductivity after heat treatment, (C) samples in which recovery in conductivity has started, while the hardness is nearly the same as the as-deformed sample, and (D) samples heat treated at 300 °C, having very high conductivity and low hardness. These points are circled and labeled in Figure 3; their microstructures are shown in Figure 4.

In Figure 4, IPF maps for samples corresponding to the points labeled A, B, C, and D in Figure 3 are shown. Visually no significant differences can be seen between figures A and B, especially for the 2.9 and 8.7 pct deformed samples though it is expected that some recovery processes must have occurred during the two-hour anneal at these temperatures. In comparison,

the microstructures for samples C clearly show larger grains as compared to both A and B, and several annealing twins are visible. Since point C was selected so that it has higher conductivity than the deformed sample but still retains high hardness, it is interesting to note that the increase in grain size has an insignificant impact on sample hardness. Grain sizes were calculated by considering all boundaries with misorientation greater than 5 deg, and hence include twin boundaries if any. We believe that since our samples contain both strained and strain-free grains, the hardness would be influenced by stored defect density in addition to the grain size. Finally, samples D have very large grains with several annealing twins in all cases. For 8.7, 12.1, and 15.9 pct deformation, conductivity of samples D is about 102 pct IACS, and hardness ranges from 30 to 40 HRF, while for the 2.9 pct deformed sample both conductivity

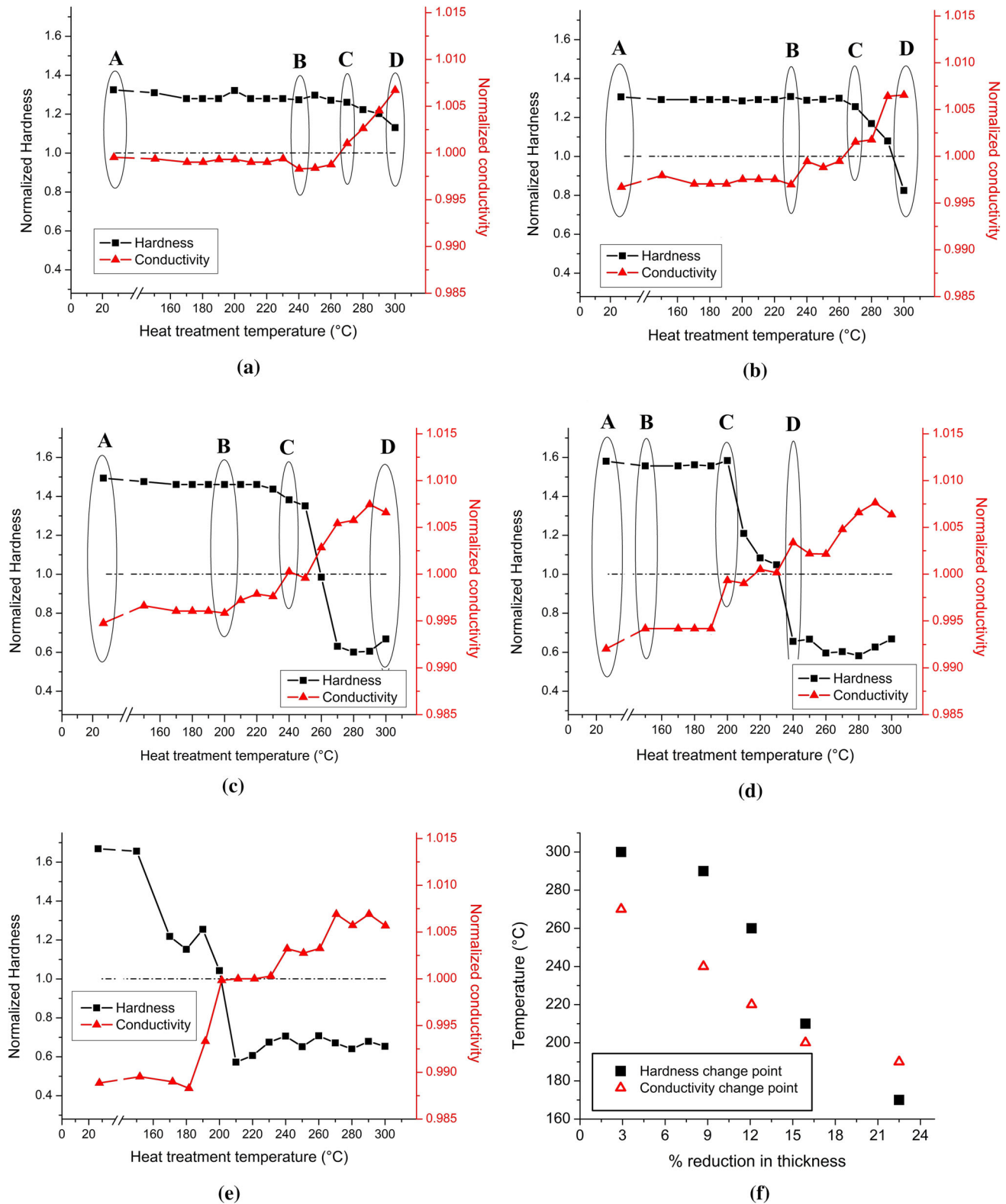


Fig. 3—The hardness and conductivity of samples deformed to (a) 2.9, (b) 8.7, (c) 12.1, (d) 15.9, and (e) 22.5 pct reduction in thickness, as a function of heat treatment temperatures. Samples A, B, C, and D have been selected to correspond to: (A) the as-deformed sample, (B) negligible change in hardness or conductivity after heat treatment, (C) sample in which recovery in conductivity has started while the hardness is nearly the same as the as-deformed sample, and (D) samples heat treated at 300 °C. The temperature at which significant change is observed in hardness and conductivity values is shown in (f). The lines joining the points are meant only as a guide to the eye.

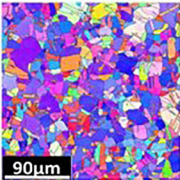
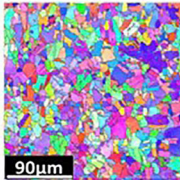
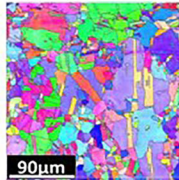
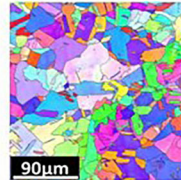
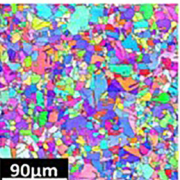
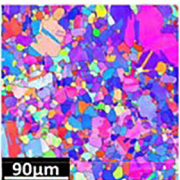
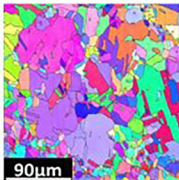
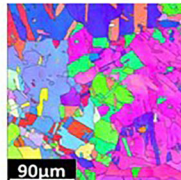
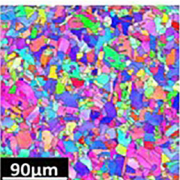
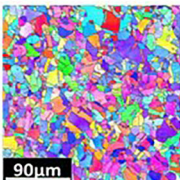
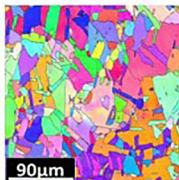
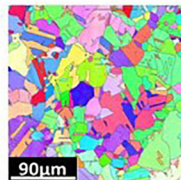
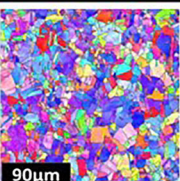
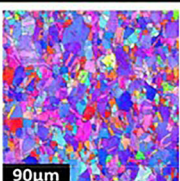
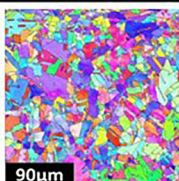
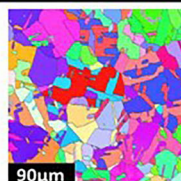
	A	B	C	D
2.9%	 90µm $11.46 \pm 2.73 \mu\text{m}$ Grains – 606	 90µm $11.73 \pm 3.50 \mu\text{m}$ Grains – 579	 90µm $20.73 \pm 5.02 \mu\text{m}$ Grains – 185	 90µm $23.26 \pm 5.23 \mu\text{m}$ Grains – 147
8.7%	 90µm $11.09 \pm 3.70 \mu\text{m}$ Grains – 647	 90µm $14.02 \pm 4.20 \mu\text{m}$ Grains – 405	 90µm $24.11 \pm 4.94 \mu\text{m}$ Grains – 137	 90µm $26.03 \pm 6.07 \mu\text{m}$ Grains – 118
12.1%	 90µm $11.70 \pm 4.05 \mu\text{m}$ Grains – 582	 90µm $11.16 \pm 4.05 \mu\text{m}$ Grains – 639	 90µm $23.30 \pm 3.30 \mu\text{m}$ Grains – 147	 90µm $25.22 \pm 5.11 \mu\text{m}$ Grains – 125
15.9%	 90µm $10.97 \pm 2.96 \mu\text{m}$ Grains – 661	 90µm $11.98 \pm 2.01 \mu\text{m}$ Grains – 555	 90µm $12.40 \pm 3.20 \mu\text{m}$ Grains – 518	 90µm $27.01 \pm 6.16 \mu\text{m}$ Grains – 109

Fig. 4—The IPF maps for points marked A, B, C, and D in Fig. 3. The colors in the IPF map denote orientations as per the standard IPF shown in Fig. 1. Each row corresponds to the percent deformation shown in first column. Column A shows the microstructure of deformed samples, while B, C, and D are for the heat treatment temperatures identified in Fig. 3. The average grain sizes, and the number of grains in the scan are shown below the microstructures.

(102 pct IACS) and hardness (about 58 HRF) are high. So it is clear that a visual examination of the microstructure is not sufficient to reveal any clear correlation between grain size and properties.

To better understand the relevant changes in microstructure that lead to the observed changes in hardness and conductivity, we have used the EBSD data. Typically, three measures of misorientation are commonly used: Grain Average Misorientation (GAM), Grain Orientation Spread (GOS), and Kernel Average Misorientation (KAM). Of these, GAM and GOS are single values defined for each grain, while KAM is calculated for each data point considering only the nearest neighboring points; for a review of these measures, see Wright *et al.*<sup>[23]</sup> A comparison of KAM, GOS, and GAM for a partially strain-free sample is

shown in Figure 5 (based on Figure 4 of Reference 24). It is clear that KAM is not suitable for distinguishing between the strain-free and strained grains in any of the samples. This, we believe, is because KAM is agnostic to grain definitions, and is more useful in the study of texture.<sup>[23]</sup> Among GOS and GAM, either can be used to compare as-deformed and completely strain-free grains. However, in partially strain-free samples, only GOS shows a sharp change at 1.1 deg, which can be used to clearly differentiate between strain-free and strained grains. Thus, we find that of the three measures, GOS is best suited to distinguish between deformed and deformation-free grains in samples that have not undergone complete recrystallization. The suitability of GOS for identifying deformation-free grains in partially recrystallized samples has been shown previously<sup>[11,25]</sup>;

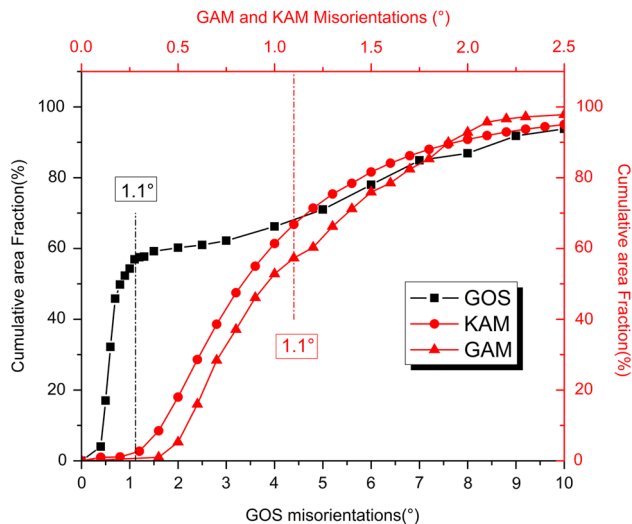


Fig. 5—The cumulative area fraction for GOS, GAM, and KAM as a function of misorientation for a partially strain-free sample.

for example, Field *et al.*<sup>[11]</sup> recommend a range of 1 to 3 deg of GOS as a cut-off to distinguish between recrystallized and deformed grains.

As indicated in the introduction section, conductivity is affected by defects such as vacancies and interstitials,<sup>[26–29]</sup> dislocations,<sup>[30–35]</sup> and grain and twin boundaries<sup>[5, 35–37]</sup>—primarily because the defects scatter the electrons and reduce the mobility of electrons by reducing the mean distance that they can travel without scatter. In our samples, as indicated above, the grain size, does not have a strong influence on the conductivity. On the other hand, GOS seems to differentiate between strained and strain-free grains and hence may also correlate well with properties that arise as a result of this “composite” microstructure. In the following, we show that this indeed is the case.

In Figure 6, we have plotted the GOS distribution for samples A, B, C, and D from Figure 3. In each case, the deformed samples show a wider spread of GOS values than heat-treated samples—with the range increasing from about 2 to 3 deg with increasing deformation. In order to bring this out more clearly, we have also plotted the FWHM in Figure 6(e). With increase in heat treatment temperature, the distribution becomes narrower and shifts to lower values of GOS, suggesting a decrease in average lattice distortion. Even for the samples labeled B in Figure 3 the GOS distribution is seen to shift to lower values, indicating a reduction in stored dislocations<sup>[11]</sup> but not enough to have any significant effect on either hardness or conductivity. Finally the GOS distribution for samples heat treated at 300 °C is very sharp with a range of about 1 degree, and with a peak below 0.5 deg, suggesting that the samples must be recrystallized.<sup>[11]</sup>

In Figure 7, we see the variation in GOS across the scanned area of the samples; grains with GOS higher than 1.1 deg are white, while those with lower GOS values are colored as per the color scale shown. The cut-off value of 1.1 deg is selected based on the observation in Figure 4 that fully annealed samples

have GOS values up to about 1 deg. GOS cut-off of 2 deg has been used in literature to identify the fraction of recrystallized grains in partially recrystallized samples.<sup>[11,25]</sup> From these figures, it is clear that with increasing percent deformation, more and more grains have values of GOS greater than 1.1 deg, and, with heat treatment, more and more grains have values of GOS less than 1.1 deg. The microstructure thus becomes a composite of deformed and deformation-free grains, impacting the measured hardness and conductivity. In fact, the analysis can be made more quantitative using area fraction of grains with GOS less than 1.1 deg as described below.

In Figure 8, we show the correlation between normalized hardness and conductivity (with respect to the hardness and conductivity of as-received samples) and area fraction of grains with GOS less than 1.1 deg (labeled  $A_{1.1}$ ). Dashed lines show the properties of the as-received samples. Interestingly, we see that when the volume fraction of the grains with low GOS is between 60 and 70 pct, both hardness and conductivity are higher than those in the as-received samples in 2.9, 8.7, and 12.1 pct deformed samples. Thus, we believe that the optimal properties are achieved by a combination of deformed and relatively deformation-free grains; deformed grains increase hardness while deformation-free grains give better conductivity. When the volume fraction of deformation-free grains (GOS less than 1.1 deg) drops below about 60 pct then conductivity of samples reduces drastically. Similarly, low hardness is measured for samples for which  $A_{1.1}$  values are greater than about 70. For the 15.9 pct deformed sample, we do not achieve the optimal fraction of about 60 to 70 pct deformation-free grains in two hours of heat treatment. The role of heat treatment time in achieving the optimal combination of properties and microstructure can be found elsewhere.<sup>[38,39]</sup> In Figure 8(e), we show the summary plot of  $A_{1.1}$  as a function of heat treatment temperature. In this figure, we have also drawn two horizontal lines to indicate regions of higher conductivity, higher hardness, and both higher hardness and higher conductivity. This plot clearly shows that the optimization of properties is achieved by tuning the fraction of deformed grains retained in the microstructure, and is achieved in an intermediate range of  $A_{1.1}$  values. Higher fractions result in an increase in hardness at the cost of conductivity and *vice versa*.

In literature on transport properties, percolation theories have been used to understand electrical conductivity for the past fifty years.<sup>[40,41]</sup> Typically it is shown that 20 to 40 volume percent (of the higher conductivity phase) leads to percolation accompanied by a steep increase in conductivity. Our aim is to retain the high conductivity of ETP copper, while enhancing its strength by thermomechanical processing—by introducing a composite microstructure of strained and strain-free grains. Thus, one might expect that at least 40 percent of strain-free grains are needed to get the appropriate conductivity. Achieving enhanced strength along with conductivity, however, as shown in Figure 8, is an optimization problem. The deformed grains in

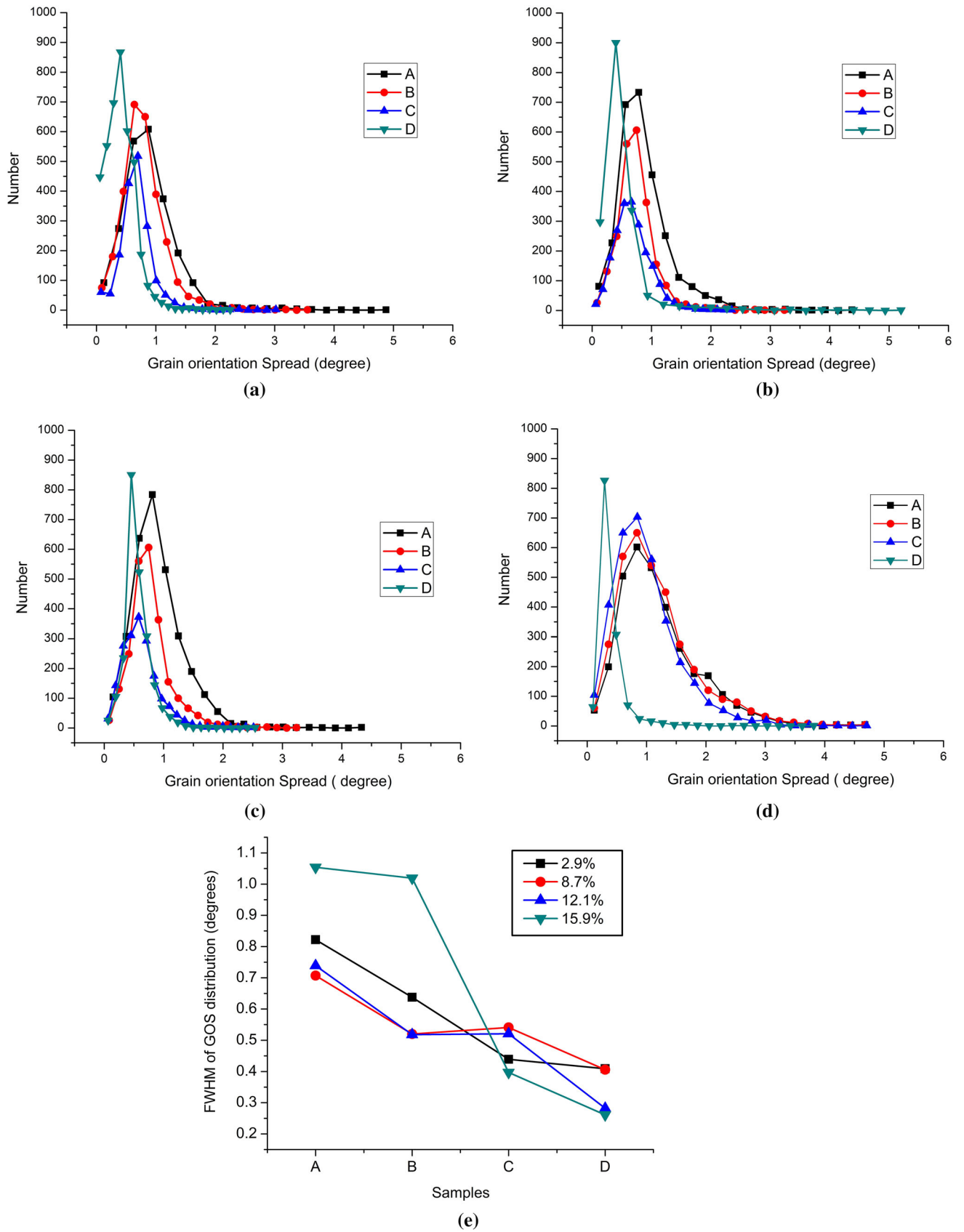


Fig. 6—The GOS distribution for samples labeled A, B, C, and D in Fig. 3, subjected to (a) 2.9, (b) 8.7, (c) 12.1, and (d) 15.9 pct deformation and subsequently heat treated. FWHM for all the samples are shown in (e). The lines joining the points are meant only as a guide to the eye.



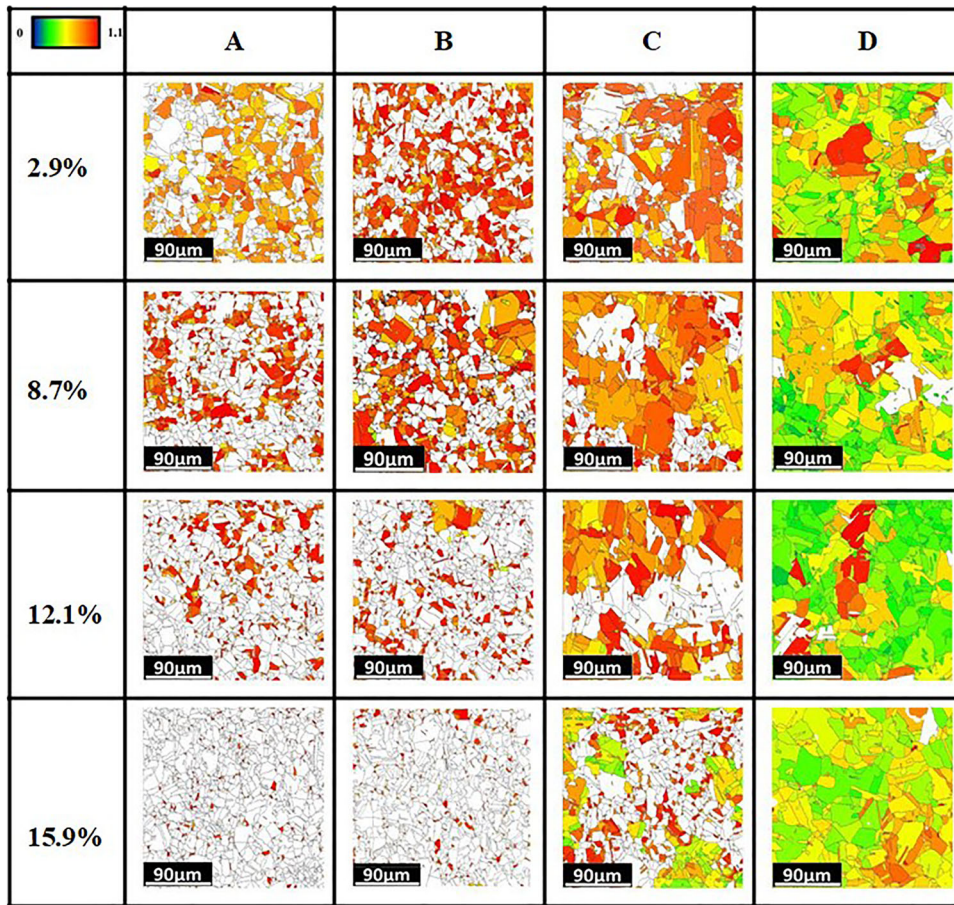


Fig. 7—The GOS maps for points marked A, B, C, and D in Fig. 3. Each row corresponds to the percent deformation shown in the first column. Column A shows the microstructure of deformed samples, while B, C, and D are samples heat treated at the temperatures shown in Fig. 3. The colors, as shown in the color bar at the top left, indicate the range of GOS between 0 and 1.1 deg. All points with GOS above 1.1 deg are colored white.

samples rolled to different percent reduction in thickness, have different hardness and conductivity because of variation in the defect density. Thus, for example, as the thickness reduction increases, high hardness can be achieved with a lower volume fraction of strain-free grains since the strained grains have higher defect density.

In Figure 9, we summarize the salient results of our study in terms of normalized hardness and conductivity values, by plotting (a) a property map and (b) a process map. Figure 9(a) shows that the combination of various percentages of deformation and heat treatment temperatures can lead to either enhancement of strength, or conductivity or both. Specifically, through appropriate choice of percent deformation and temperature for heat treatment, it is possible to obtain simultaneous enhancement of both hardness (to about 20 pct over the as-received value) and conductivity (to about 0.6 pct on the as-received value). Such samples fall in quadrant one of Figure 9(a) and are obtained by deforming the samples to less than 10 pct and annealing for two hours in the temperature range 270 °C to 300 °C. The thermomechanical process used by us to achieve the optimum microstructure and hence the desired properties is similar to strain recrystallization<sup>[9]</sup>; however,

strain recrystallization typically involves heat treatment at higher temperatures and for shorter times than those in our study. In order to show the range of deformation and the corresponding heat treatment temperature range, we have plotted a process map in Figure 9(b). The preferred processing range corresponding to quadrant one in 9a is shown by filled symbols in Figure 9(b).

Further, if a decrease of about 0.01 pct in conductivity is acceptable, the hardness can be increased up to about 60 pct of the as-received value; in a similar fashion, if a decrease of about 20 pct in hardness is acceptable, the conductivity can be increased up to 0.6 pct over the as-received value. Samples with higher hardness and lower conductivity than as received are in quadrant four, while those with lower hardness and higher conductivity are in quadrant two of Figure 9(a).

Even though we have identified the processes that help us obtain higher strength without changes in conductivity, further studies are needed to understand the stability of the microstructure consisting of strained and strain-free grains during service conditions, and, the fatigue response of such a composite microstructure. The results of such studies are crucial from a practical point of view.

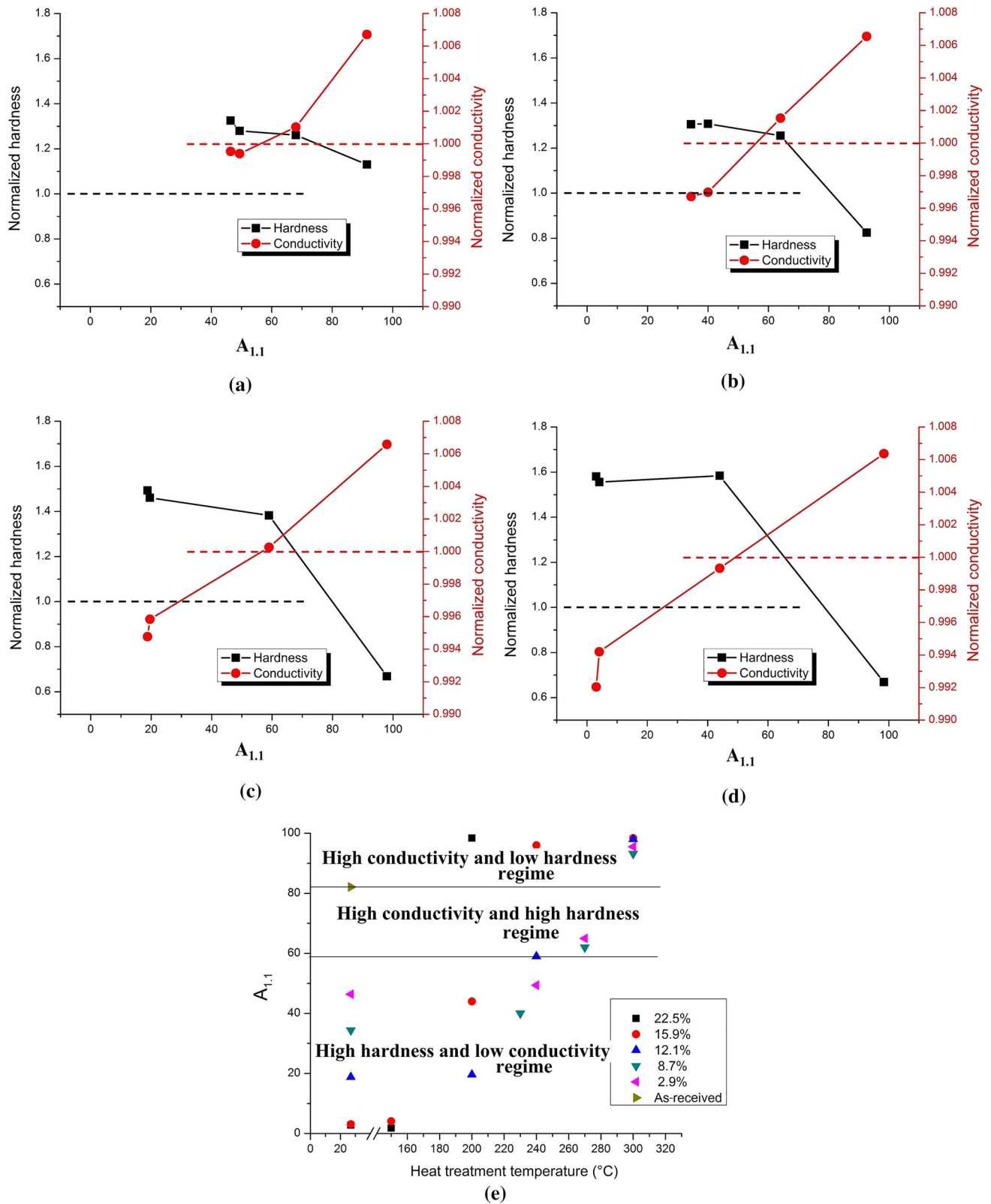


Fig. 8—The normalized hardness and conductivity (with respect to as-received samples) for samples A, B, C, and D as a function of area fraction of strain-free grains with GOS less than 1.1 deg ( $A_{1,1}$ ) for (a) 2.9, (b) 8.7, (c) 12.1, and (d) 15.9 pct reduction in thickness, followed by heat treatment. The lines joining the points are meant only as a guide to the eye. (e) Summary plot of  $A_{1,1}$  versus heat treatment temperature. The two lines indicate the optimal range for  $A_{1,1}$  values that lead to both higher conductivity and hardness relative to as-received samples.

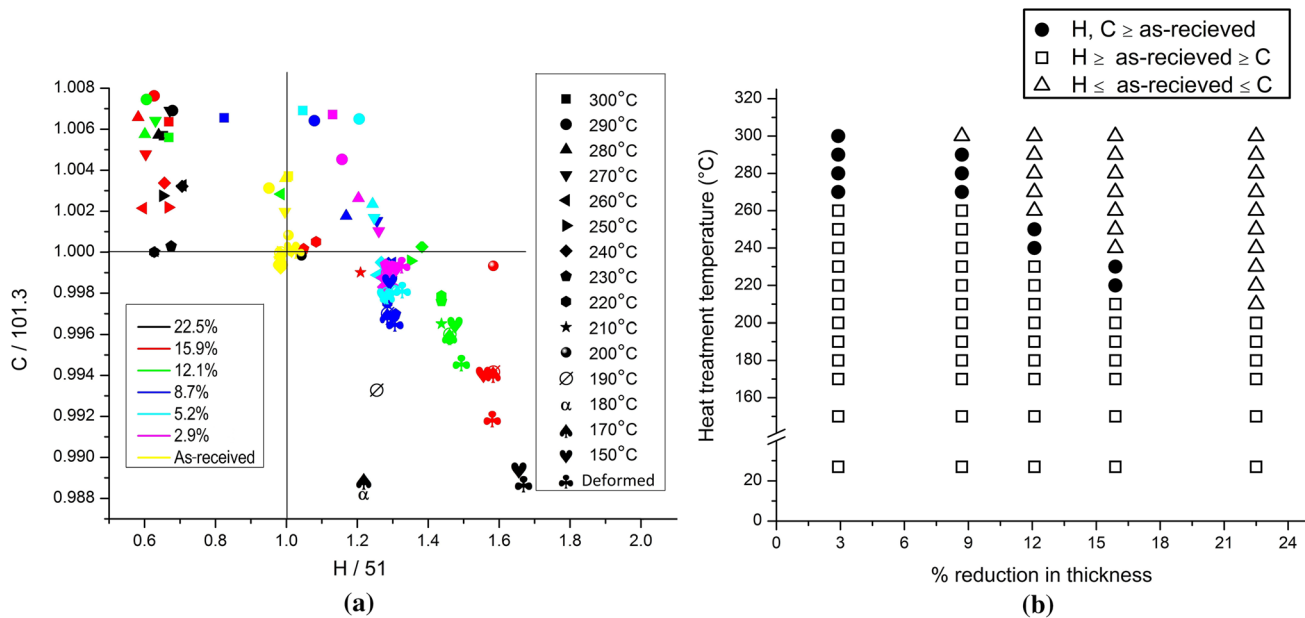


Fig. 9—(a) The plot of normalized hardness versus normalized conductivity for samples that have undergone various amounts of deformation and heat treated at different temperatures. The normalization is carried out using the values for the as-received samples. In the legend, the percent values represent reduction in thickness; temperatures indicate two-hour heat treatment at the mentioned temperature. (b) Process map showing the dependence of properties on percent deformation and heat treatment temperature. The filled symbols show the preferred process parameter range where both hardness and conductivity are enhanced.

#### IV. CONCLUSIONS

- Rolling up to about 23 pct reduction followed by extensive heat treatment (up to temperature below  $0.5T_m$ ) was carried out on LME Grade A copper strips. After 2 hours of heat treatment, it is possible to either enhance hardness or conductivity up to 60 and 0.6 pct, respectively.
- We have found that among the various measures of misorientation, GOS shows the best correlation with hardness and conductivity, for samples deformed up to 23 pct. This, we believe, is because of the ability of GOS to distinguish between deformed and relatively deformation-free grains.
- We have identified the microstructural features that contribute to hardness and/or conductivity enhancement; specifically, a combination of deformed and relatively deformation-free grains is responsible for the optimal hardness and conductivity. We show that a minimum of 30 to 40 pct of deformed grains is essential for obtaining a combination of hardness and conductivity values higher than as-received sample (51 HRF and 101.3 pct IACS).

#### ACKNOWLEDGMENTS

We thank Crompton Greaves Company for funding this project and for supplying the ETP copper samples and Dr. Janamejay Nemade, formerly of Crompton

Greaves Company for useful discussions. EBSD studies were carried out at the National Facility of Texture and OIM—a DST-IRPHA facility.

#### REFERENCES

1. Chapman: Copper Development Association Publication No. 122 and European Copper Institute Publication No. Cu0232, 1998.
2. J.R. Davis: *ASM Speciality Handbook*, ASM International, Materials Park, 2001.
3. C. Kittel: *Introduction to Solid State Physics*, Wiley, New York, 2004.
4. Y. Zhang, Y.S. Li, N.R. Tao, and K. Lu: *Appl. Phys. Lett.*, 2007, vol. 91, pp. 10–13.
5. L. Lu, Y. Shen, X. Chen, L. Qian, and K. Lu: *Science*, 2004, vol. 304, pp. 422–26.
6. A. Habibi, M. Ketabchi, and M. Eskandarzadeh: *J. Mater. Process. Technol.*, 2011, vol. 211, pp. 1085–90.
7. A. Habibi and M. Ketabchi: *Mater. Des.*, 2012, vol. 34, pp. 483–87.
8. O.F. Higuera-Cobos and J.M. Cabrera: *Mater. Sci. Eng. A*, 2013, vol. 571, pp. 103–14.
9. M. Kumar, W.E. King, and A.J. Schwartz: *Acta Mater.*, 2000, vol. 48, pp. 2081–91.
10. P. Zhang, S.X. Li, and Z.F. Zhang: *Mater. Sci. Eng. A*, 2011, vol. 529, pp. 62–73.
11. D. Field, L. Bradford, M. Nowell, and T. Lillo: *Acta Mater.*, 2007, vol. 55, pp. 4233–41.
12. J.G. Thompson: *Natl. Bur. Stand.*, 1934, vol. 13, pp. 745–56.
13. N. Hansen and T. Leffers: *Rev. Phys. Appl.*, 1988, vol. 23, pp. 519–31.
14. V.S. Ananthan, T. Leffers, and N. Hansen: *Mater. Sci. Technol.*, 1991, vol. 7, pp. 1069–75.
15. N. Hansen: *Scr. Metall.*, 1992, vol. 27, pp. 1447–52.
16. O.V. Mishin and G. Gottstein: *Philos. Mag. A*, 1998, vol. 78, pp. 373–88.
17. N. Hansen: *Metall. Mater. Trans. A*, 2001, vol. 32A, pp. 2917–35.
18. T. Leffers, V.S. Ananthan, and H. Christoffersen: *Mater. Sci. Eng. A*, 2001, vols. 319–321, pp. 148–51.
19. L. Lu, M.L. Sui, and K. Lu: *Acta Mater.*, 2001, vol. 49, pp. 4127–34.

20. S. Suwas, A.K. Singh, K.N. Rao, and T. Singh: *Zeitschrift für Met.*, 2003, vol. 93, pp. 918–27.
21. G. Benchabane, Z. Boumerzoug, T. Gloriant, and I. Thibon: *Phys. B Condens. Matter*, 2011, vol. 406, pp. 1973–76.
22. L. Lapeire, J. Sidor, P. Verleysen, K. Verbeken, I. De Graeve, H. Terryn, and L.A.I. Kestens: *Acta Mater.*, 2015, vol. 95, pp. 224–35.
23. S.I. Wright, M.M. Nowell, and D.P. Field: *Microsc. Microanal.*, 2011, vol. 17, pp. 316–29.
24. N. Harshavardhana, G. Kumar, and A.K. Saxena: *Bull. Mater. Sci.* (manuscript under review).
25. T. Konkova, S. Mironova, A. Korznikov, and S.L. Semiatin: *Mater. Sci. Eng. A*, 2011, vol. 528, pp. 7432–43.
26. C.J. Meechan and J.A. Brinkman: *Phys. Rev.*, 1956, vol. 103, pp. 1193–1202.
27. R. Losehand, F. Rau, and H. Wenzl: *Radiat. Eff.*, 1969, vol. 2, pp. 69–74.
28. O. Buck, D. Schumacher, and A. Seeger: *Basic Solid State Phys.*, 1973, vol. 707, pp. 707–11.
29. W. Schuele: *Tech. Report, Jt. Res. Centre, Eur. Commun. Inst. Adv. Mater.*, 1994.
30. H. Yoshinaga: *Basic Solid State Phys.*, 1966, vol. 18, pp. 625–36.
31. Y. Chang and R. Higgins: *Phys. Rev. B*, 1975, vol. 12, pp. 4261–81.
32. K.M. Mannan and K.R. Karim: *J. Phys. F Met. Phys.*, 1975, vol. 5, pp. 1687–93.
33. Z.S. Basinski, M. Sahoo, and S. Saimoto: *Acta Metall.*, 1977, vol. 25, pp. 657–65.
34. Z.S. Basinski and J.S. Dugdale: *Phys. Rev. B*, 1985, vol. 32, pp. 2149–55.
35. T.H. Blewitt, R.R. Coltman, and J.K. Redman: *Phys. Rev.*, 1954, vol. 4, p. 891.
36. I. Nakamichi: *Mater. Sci. Forum*, 1996, vols. 207–209, pp. 47–58.
37. W. Yan, J. Chen, and X.H. Fan: *Nonferrous Metals Soc. China*, 2003, vol. 13, pp. 1075–79.
38. N. Harshavardhana: PhD thesis, Indian Institute of Technology Bombay, Mumbai, India, 2017.
39. N. Harshavardhana, M.P. Gururajan, and P. Pant: Manuscript under preparation.
40. S. Kirkpatrick: *Rev. Mod. Phys.*, 1973, vol. 45, pp. 574–88.
41. I. Webman, J. Jortner, and M.H. Cohen: *Phys. Rev. B*, 1975, vol. 11, pp. 2885–92.

**Publisher's Note** Springer Nature remains neutral with regard to jurisdictional claims in published maps and institutional affiliations.